Proceedings of 5th Jagiellonian Symposium on Advances in Particle Physics and Medicine, Kraków, Poland, 2024

Modelling the Effect of Neutron Damage on Low-Gain Avalanche Detectors

C. Jain[a,*], K. Tiwari[a], T. Kumar[a], M. Sharma[a], S. Phor[a], A. Kumar[a], N. Agrawal[b], K. Ranjan[a] and A. Bhardwaj[a]

[a] *CDRST, Department of Physics and Astrophysics, University of Delhi, North Campus, Delhi 11007, New Delhi, India*
[b] *Swami Shraddhanand College, University of Delhi, Delhi 110036, New Delhi, India*

Doi: 10.12693/APhysPolA.146.725 *e-mail: chakresh.jain@cern.ch

Low-Gain Avalanche Detectors are pivotal for the advancement of future nuclear, particle, and astroparticle experiments due to their exceptional fast timing capabilities and radiation hardness. Studying the performance of these detectors under adverse radiation environments is of significant importance, both from the fabrication and modelling point of view. This research aims to develop a reliable neutron-induced radiation damage model specifically for Low-Gain Avalanche Detectors using the technology computer-aided design simulator, Silvaco. The capabilities of the neutron damage model in Silvaco, originally developed by our group for pad detectors, are enhanced further by incorporating the acceptor removal mechanism, thus making it applicable to both thin and thick Low-Gain Avalanche Detectors. Validating this model is essential to ensure the reliability and performance of Low-Gain Avalanche Detectors in high-radiation environments, thereby supporting their integration into next-generation collider experiments.

topics: solid state detectors, silicon detectors, Low-Gain Avalanche Detectors (LGADs), radiation hardness

1. Introduction

The High-Luminosity phase of the Large Hadron Collider (HL-LHC) will start in 2029, operating at (5–7.5) $\times$ 10^{34} cm^{-2} s^{-1} luminosities, increasing average hard proton–proton interactions to 140–200, and at higher radiation levels for ATLAS (A Toroidal LHC ApparatuS) and CMS (Compact Muon Solenoid) detectors [1, 2]. Current detectors, designed for lower radiation, will struggle to accurately assign reconstructed tracks to their primary interaction vertices, which necessitates precise timing information for individual tracks. To meet the stringent requirements of HL-LHC experiments, it is crucial to upgrade to more efficient and radiation-hard silicon detectors [3, 4].

Traditional silicon sensors, while having high spatial granularity, struggle with accurate particle arrival timing, typically achieving timing resolution of the order of 200 ps [5]. Thinner sensors offer better radiation hardness and lower power consumption but suffer from signal reduction and relatively larger noise, thus lowering the signal-to-noise ratio (SNR). High fluences further reduce SNR, limiting the sensors' effectiveness in the HL-LHC phase.

A relatively novel configuration of silicon detectors, Low-Gain Avalanche Detectors (LGADs), are promising for high-radiation environments. LGADs are p-bulk-based n$^+$–p diodes with a p-type gain layer beneath the n$^+$ implant. Under reverse bias, they create a high electric field region (p-well) for avalanche multiplication, enhancing SNR even under high irradiation [5–8]. Thin sensors ($\sim$ 50 μm) with internal gain ($\sim$ 20) offer about 10 ps time resolution [5]. LGADs, with fast response and high SNR, are already used in the Phase-2 upgrade of the ATLAS's High-Granularity Timing Detector (HGTD) and CMS's Minimum Ionizing Particle (MIP) Timing Detector (MTD) [9–12].

TCAD (technology computer-aided design) simulations are vital for developing radiation–resistant structures. The University of Delhi (DU) team developed radiation damage models for proton [13] as well as neutron [14] irradiations using Silvaco TCAD [15]. Both of these models consist of two bulk traps — an acceptor and a donor — to analyze full depletion voltage (V_{FD}), leakage current (I_{LEAK}), and charge collection efficiency (CCE). In addition, modelling is also done for surface charge density (Q_F) and interface traps (N_{it}) to take care of the ionizing nature of proton irradiation. The

TABLE I

Values of different design parameters of LGAD, neutron radiation environment, and operating temperature used in simulations.

LGAD design parameter	Value
Thickness	300 μm
Active thickness	246 μm
Width	80 μm
p-bulk doping density, N_b (1×10^{12} cm^{-3})	1.33
p-well peak concentration, N_p (1×10^{16} cm^{-3})	7.68
p-well doping depth, D_p	6 μm
n$^+$ implant peak concentration, N_n (1×10^{18} cm^{-3})	1
n$^+$ implant doping depth, D_n	2.945 μm
Neutron fluence (1 MeV n$_{eq}$/cm^{-2})	up to 2×10^{15}
Temperature	253 and 263 K

validity of these models has been tested by reproducing a wide variety of experimental data from irradiated diodes and strips. Previous work using Silvaco TCAD studied proton-irradiated LGADs with various doses and thicknesses, aiming to optimize designs for proton irradiation using DU's two-trap bulk proton radiation damage model [16, 17]. The proton damage model was also validated by the experimental observations under the Hamamatsu Photonics K.K. (HPK) campaign, which resulted in a change of polarity (from n-type to p-type) of silicon detectors proposed for the HL-LHC phase [18].

This paper extends the previous neutron damage modelling work by applying the neutron radiation damage model to thick (300 μm) LGADs using Silvaco TCAD [15]. Since the original model was developed for PIN diodes, it does not account for two possible effects observed in LGADs, namely the acceptor removal mechanism in the gain layer and the impact ionization behaviour of the gain layer, which are shown to be significant aspects resulting in limiting the gain of LGAD at higher fluences [19]. In the present simulations, an analytical model of p-well doping has been used along with the developed neutron damage model to simulate the acceptor removal mechanism [20] to replicate the real device behaviour. It is to be noted that recent TCAD works show limited agreement between simulations and experiments due to challenges in the implementation of precise device model for electric field profiles [21–24]. Considering this, the impact ionization coefficients are tuned to improve the simulation–measurement agreement, validating the neutron damage model for optimizing radiation-hard LGAD designs, which is crucial for HL-LHC environments. It is also worth mentioning that the simulation results on LGADs presented in this work can, in general, be useful for the development of neutron detectors also used in medical applications such as boron neutron capture therapy, as discussed in [25, 26].

2. Device structure and parameters

TCAD simulations are based on the measurement data from 300 μm thick, non-irradiated, and neutron-irradiated LGAD structures with different design parameters. The values of two parameters, active thickness and p-bulk doping density (N_b), have been fixed using the saturation value of $1/C^2$ vs V plot (where C is the capacitance) and the slope of the linear portion between gain layer voltage (V_{GL}) and full depletion voltage (V_{FD}) extracted from experimental capacitance–voltage (C–V) characteristics of non-irradiated LGAD given in [6]. On the other hand, the value of V_{GL} and charge collection (CC) of the un-irradiated LGAD are used to determine the value of the other four parameters: p-well peak concentration (N_p), p-well doping depth (D_p), n$^+$ implant peak concentration (N_n), n$^+$ implant doping depth (D_n). As the charge collection is very sensitive to the changes in these parameters, their optimization requires careful sensitivity studies within a certain range of parameters. The set of values chosen in the parameter phase space, obtained from sensitivity studies, describe the simulation results, which are in agreement with the available measurement results of [6]. Table I summarizes these design parameters along with the radiation environment and operating temperature. The simulations are performed for a neutron fluence up to 2×10^{15} MeV n$_{eq}$/cm^2 and at two different temperatures, $T = 253$ K and $T = 263$ K, according to the available measurement data.

Simulations use a two-dimensional geometry and Gaussian profiles for front-side and back-side implants. The front-side implant's peak concentration and junction depth are tuned based on measurements. For the back-side implant, a deep diffused boron implantation with a peak concentration of 1×10^8 cm^{-3} is used. Capacitance–voltage (C–V) characteristics use a 1 kHz alternating current (AC) signal. The Selberherr model is employed for impact ionization. Figure 1a shows the 1D doping profile of both acceptor (p-well and p-bulk) and donor (n$^+$) concentrations, as well as the absolute net doping profile developed in LGAD. The resultant junction formed between the n$^+$ implant and p-well results in a high electric field, which helps in charge multiplication in the p-well. To illustrate the effect of the doping profile of LGAD, Fig. 1b shows 2D electric field contours developed within the LGAD structure on the application of a reverse bias voltage of 300 V.

TABLE II

Neutron radiation damage model used in simulations [14].

Trap type	Energy level [eV]	$G_{\mathbf{int}}$ [cm^{-1}]	σ_e [cm^2]	σ_h [cm^2]
Acceptor	$E_C - 0.51$	4	9×10^{-15}	3.8×10^{-14}
Donor	$E_V + 0.48$	1	1×10^{-14}	1×10^{-14}

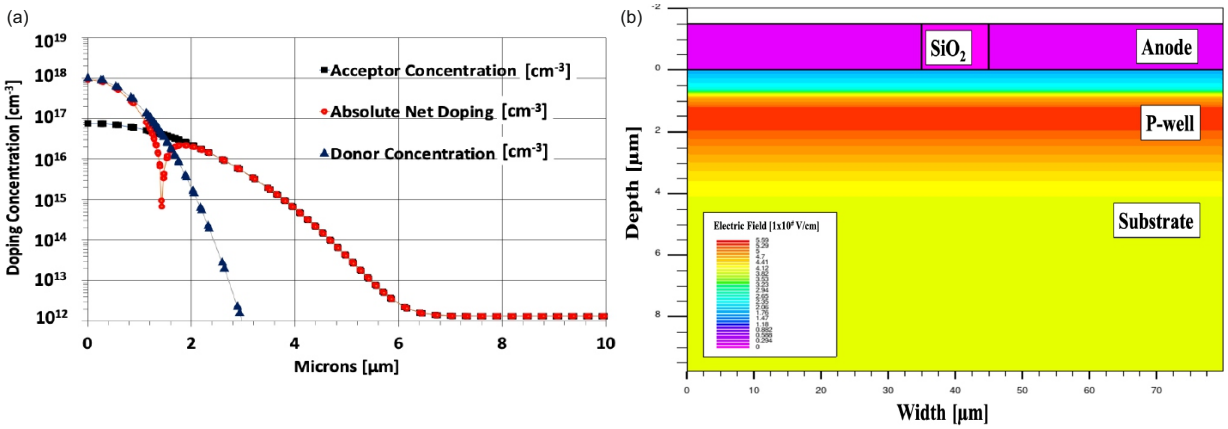

Fig. 1. (a) Doping profiles developed in LGAD. (b) 2D electric field distribution in a simulated LGAD structure at 300 V near the junction (up to 10 μm depth).

It also schematically represents the different regions of LGAD structure such as: "SiO_2", "Anode", "P-well", and "Substrate". The colour scheme shows that a high electric field is developed in the p-well region (represented by red colour) near the front-end electrode (Anode). The strength of the electric field then decreases sharply, which is represented by a transition from a red colour contour to a yellow colour contour as the distance in bulk increases from the p-well to the substrate region.

Charge collection efficiency (CCE) is assessed using the transient current technique (TCT) method. An infrared laser pulse of 2 W power and 1 μm width with a wavelength of 1060 nm generates a transient signal. The metal contacts are removed from the entry and exit points and replaced with SiO_2 to avoid laser reflection. TCT simulations use mixed-mode simulations with external circuit elements, i.e., a bias tee with 3.1 kΩ resistance and 2.2 nF capacitance.

3. Neutron radiation damage model

Irradiation of silicon detectors with hadrons induces various kinds of defects in the silicon lattice. These defects create various trap levels in the forbidden energy gap of the silicon, altering the detector's macroscopic behaviour. In our previous studies, it has been demonstrated that these irradiation effects can be effectively parameterized using a radiation damage model consisting of only a few trap energy levels, which effectively represent the impact of all real traps. These models incorporate two bulk traps, surface charge density, along with two interface traps in the case of proton irradiation [13] and only two bulk traps in the case of neutron irradiation [14]. Each trap level is defined by the following parameters: trap type (acceptor or donor), energy level relative to the conduction (E_C) or valence band (E_V), the introduction rate of the trap (G_{int}), and electron/hole capture cross-sections (σ_e, σ_h). The introduction rate G_{int} estimates trap density (n_t) using $n_t = G_{int}\Phi$, where Φ is the irradiation fluence. In our simulations, we assume a uniform distribution of both acceptor and donor traps within the bulk of the sensor.

In the present work, the neutron radiation damage model is used to implement the effects of neutron irradiation on LGADs along with gain layer degradation modelling, as described in the next section. This simplified model accurately reproduces key detector parameters such as leakage current (I_{LEAK}), full depletion voltage (V_{FD}), charge collection efficiency (CCE), and trapping probability in neutron-irradiated silicon sensors, particularly in reference devices without an additional multiplication layer. The credibility of the developed neutron radiation damage model in the case of traditional silicon sensors is evidenced by [14].

Table II lists the optimized values for various trap parameters, including energy levels, introduction rates for neutron radiation-induced traps, and electron/hole capture cross-sections (σ_e/σ_h).

It is to be noted that the neutron damage model does not include the effects of surface damage, which is primarily caused by ionizing radiation.

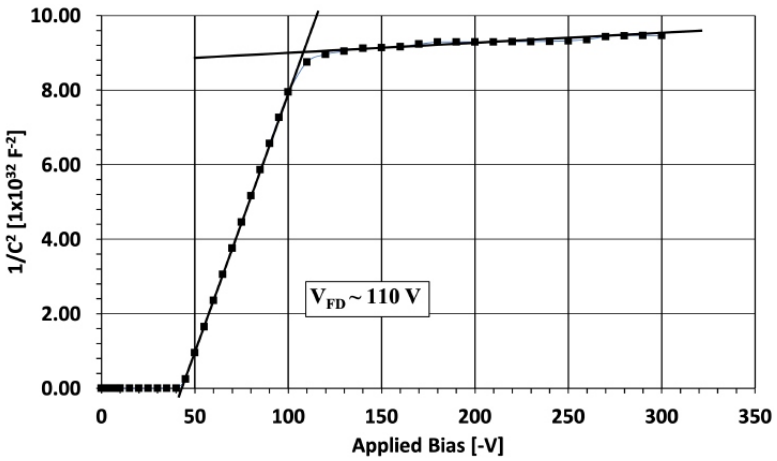

Fig. 2. Simulated $1/C^2$ versus applied bias ($-V$) plots for non-irradiated LGAD at 293 K.

4. Gain layer degradation

Neutron irradiation damages the bulk of LGADs, affecting their performance analogously to traditional silicon detectors. This is modelled using the aforementioned damage model. Additionally, LGADs experience the acceptor removal mechanism at high neutron fluence, particularly in the p-type gain layer, known as gain layer degradation. This reduces effective doping concentration and electric field strength, limiting gain and performance at higher fluences. While the damage model explains silicon detector damage, it does not account for the acceptor removal mechanism effectively in the gain layer. To simulate this in LGADs, analytical modelling of the p-well concentration is used as a function of hadron fluence to reflect LGAD behaviour under high radiation [20]. According to the analytical modelling, the initial acceptor concentration in the p-well region decreases exponentially with the irradiation fluence as given by

$$N_A = N_{A,0}\, \mathrm{e}^{-c\Phi_{eq}}, \tag{1}$$

where Φ_{eq} is the incident fluence, $N_{A,0}$ is the initial acceptor concentration, N_A is the acceptor concentration at fluence Φ_{eq}, and c is an acceptor removal constant.

The value of "c" and the impact ionization coefficients have been parameterized to fit the experimental results.

5. Results

5.1. Capacitance–voltage characteristics

To cross-check the LGAD parameters used in the simulations, the bulk capacitance of non-irradiated LGAD is simulated. Figure 2 shows the simulated results for the inverse square bulk capacitance of a non-irradiated LGAD as a function of reverse bias voltage. The simulations are performed at 293 K to match the experimental conditions. The simulated results reproduce the measurement behaviour where capacitance changes only slightly until p-well depletion corresponds to V_{GL}. The simulated $V_{FD} \simeq$ 110 V is found to be consistent with the measured values of 90–120 V, as clearly inferred from the measurement plot published in [6], where measurements were performed on several LGADs from the same wafer at 293 K. The extracted values of V_{GL} and V_{FD} from the experimental C–V characteristics of [6] were used to determine bulk doping density and active thickness used in simulations. The C–V characteristics from simulations agree well with measurements [6].

5.2. Leakage current variation

Figure 3 shows the simulated leakage current behaviour of an LGAD with increasing reverse bias voltage for both non-irradiated and neutron-irradiated conditions. The I_{LEAK} values are simulated at 263 K for non-irradiated and at 253 K for irradiated LGADs so that results can be compared against the available measurements [6]. Unlike traditional silicon detectors, where the current saturates after full depletion, the leakage current in LGADs increases continuously due to charge multiplication. The behaviour of simulated leakage current (I–V characteristics) agrees qualitatively with the experimental results, as presented in [6]. Yet, the values of leakage current differ from the experimental values due to differences in surface area of the experimental structure and simulated geometry. However, a slight discrepancy is observed between the simulated and measured current behaviour at a fluence of 2×10^5 1 MeV $\mathrm{n}_{eq}/\mathrm{cm}^2$ at low voltages up to 500 V, which requires further understanding and more optimized modelling of the damaging effects of neutrons on LGADs at high fluences.

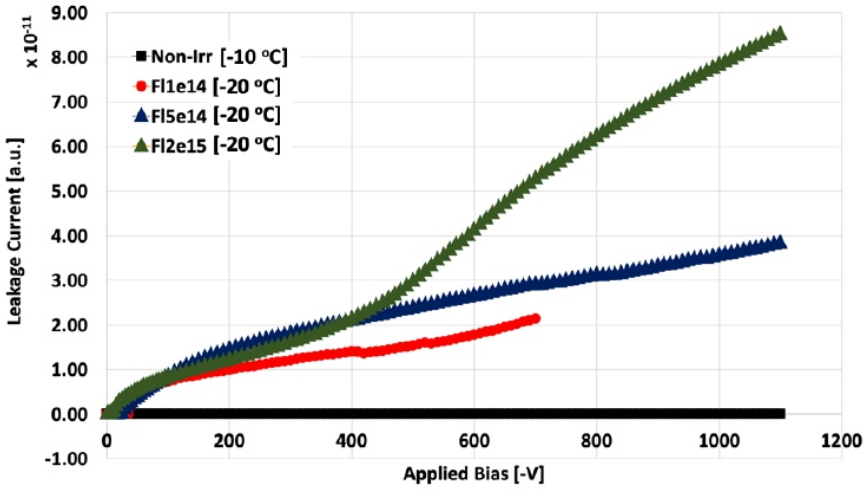

Fig. 3. Variation of simulated values of I_{LEAK} with applied bias voltage for a non-irradiated as well as neutron irradiated LGAD for three different fluence values: 1×10^{14} 1 MeV n_{eq}/cm^2, 5×10^{14} 1 MeV n_{eq}/cm^2, and 2×10^{15} 1 MeV n_{eq}/cm^2. The current is plotted in arbitrary units (a.u.).

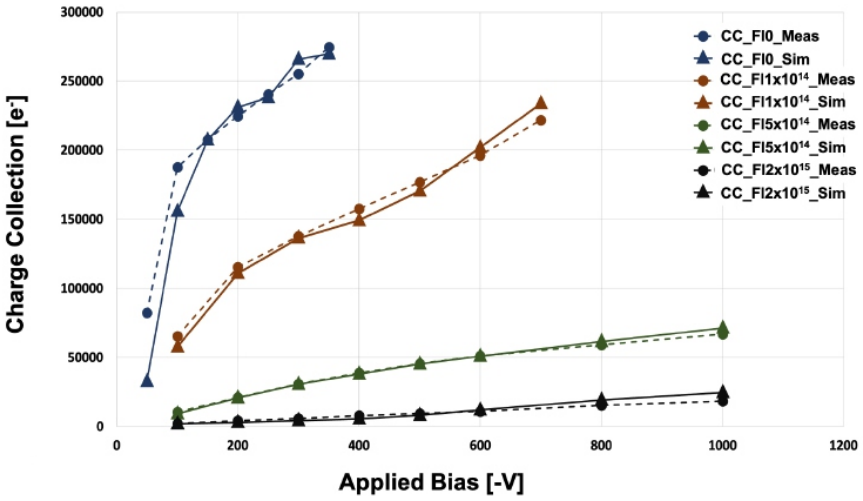

Fig. 4. Variation of simulated and measured charge collection with applied bias voltage for an LGAD at different neutron fluences. The experimental values are taken from [6].

5.3. Charge collection variation

The neutron radiation damage model (Table II) with acceptor removal in the gain layer is used to simulate LGADs under neutron irradiation. Simulations are performed at 263 K for non-irradiated LGADs and 253 K for irradiated ones, at different neutron fluences of 1×10^{14}, 5×10^{14}, and 2×10^{15} 1 MeV $n_{eq}/cm2$ [6]. The collected charge is calculated by integrating the transient signal and standardised for traditional silicon detectors with 24000 electrons as the total charge collected after full depletion.

Figure 4 compares collected charge versus bias voltage for non-irradiated and irradiated LGADs. As expected, the charge increases with bias and decreases with neutron fluence. Simulations align with experimental results, validating that neutron irradiation reduces acceptor concentration in the p-well, lowering the electric field and, hence, charge multiplication. Gain remains above 1 for non-irradiated LGADs and for irradiation levels up to 1×10^{14} 1 MeV n_{eq}/cm^2. For 5×10^{14} 1 MeV n_{eq}/cm^2, gain is above 1 only at bias voltages more than 300 V. At 2×10^{15} 1 MeV n_{eq}/cm^2, gain remains lower than 1 up to 1500 V, as observed experimentally.

Although the overall trend of simulation results tends to agree with measurement results for all the fluence values, certain discrepancies in current at high fluences and CCE values seem to suggest further optimization of the neutron damage model for LGADs.

6. Conclusions

This work is an effort to widen the scope of the existing neutron radiation damage model for LGADs. In addition to the bulk damage model, an acceptor removal mechanism is also implemented in TCAD simulations to incorporate the effects of neutron irradiation on LGAD structures. The study highlights the impact of neutron radiation on LGAD performance. Simulations at various temperatures (253 and 263 K) and for neutron fluence levels up to 2×10^{15} 1 MeV n_{eq}/cm^2 reveal significant degradation in the gain layer due to acceptor removal. This leads to reduced effective doping concentration, lower electric field strength, decreased charge collection efficiency (CCE), and increased leakage current (I_{LEAK}). The results are in close agreement with the experimental results and provide valuable insights for optimizing LGAD design to enhance radiation tolerance, demonstrating the complex relationship between neutron irradiation and LGAD performance.

Acknowledgments

The authors would like to thank the University of Delhi for providing infrastructure support and the Department of Science and Technology (DST) for providing financial assistance.

References

[1] High-Luminosity Large Hadron Collider (HL-LHC): Technical design report, *CERN Yellow Reports: Monographs*, CERN, Geneva (2020).

[2] *High-luminosity large hadron collider (HL-LHC): Technical design report v.0.1*, 2017.

[3] A MIP Timing Detector for the CMS Phase-2 Upgrade, Technical Design Report, CERN-LHCC-2019-003; CMS-TDR-020.

[4] *Technical Proposal for a MIP Timing Detector in the CMS Experiment Phase-2 Upgrade*, CERN-LHCC-2017-027; CMS-P-009.

[5] H.F.-W. Sadrozinski, A. Seiden, N. Cartiglia, *Rep. Progr. Phys.* **81**(2), 026101 (2017).

[6] G. Pellegrini et al., *Nuclear Instruments and Methods in Physics Research A* **765**, 12 (2014).

[7] N. Cartiglia et al., *Nuclear Instruments and Methods in Physics Research A* **796**, 141 (2015).

[8] M. Mandurrino, Silicon detectors for the LHC Phase-II upgrade and beyond. RD50 status report, 2019, arXiv:1910.06045.

[9] ATLAS Collaboration, Technical Proposal: A High-Granularity Timing Detector for the ATLAS Phase-II Upgrade, *Tech. Rep. CERN-LHCC-2018-023. LHCC-P-012*, CERN, Geneva (Jun, 2018).

[10] CMS Collaboration, Technical proposal for a MIP timing detector in the CMS experiment phase 2 upgrade, *Tech. Rep. CERN-LHCC-2017-027. LHCC-P-009*, CERN, Geneva (Dec, 2017).

[11] ATLAS collaboration, Technical Design Report: A High-Granularity Timing Detector for the ATLAS Phase-II Upgrade, Tech. Rep. CERN-LHCC-2020-007, ATLAS-TDR-031, CERN, Geneva (2020).

[12] C. CMS, A MIP Timing Detector for the CMS Phase-2 Upgrade, Tech. Rep. CERN-LHCC-2019-003, CMS-TDR-020, CERN, Geneva (2019).

[13] R. Dalal et al., In: *Proc. Sci. (Vertex)* **227**, 030 (2014).

[14] C. Jain, S. Saumya, G. Jain, R. Dalal, N. Agrawal, A. Bhardwaj, K. Ranjan, *Semicond. Sci. Technol.* **35**, 045021 (2020).

[15] ATLAS Silvaco version 8.2.12.R 2012 Users Manual (Santa Clara: SILVACO, Inc) pp. 621–80.

[16] R. Dalal et al., *Nucl. Instrum. Methods Phys. Res. A* **836**, 113 (2016).

[17] G. Jain, C. Jain, S. Saumya, N. Agrawal, A. Bhardwaj, K. Ranjan, *Semicond. Sci. Technol.* **36**, 065016 (2021).

[18] W. Adam et al., *JINST* **12**, P06018 (2017).

[19] E. Curras Rivera et al., *JINST* **18**, P10020 (2023).

[20] G. Kramberger, et al., *JINST* **10**, P07006 (2015).

[21] M. Mandurrino et al., in: *2017 IEEE Nuclear Science Symposium and Medical Imaging Conference (NSS/MIC)*, pp. 1–4.

[22] T. Croci, et al., *JINST* **17**, C01022 (2022).

[23] T. Yang et al., *Tech. Rep.* **140, 167111 (2021)**.

[24] E. Curras, M. Moll, *IEEE Transactions on Electron Devices* **70**(6), 2023).

[25] W. Sauerwein, T. Fischer, L. Sancey et al., *BAMS* **19**, 48 (2023).

[26] A. Khreptak, M. Skurzok, *BAMS* **19**, 74 (2023).